International Symposium
On Turbulence and Shear Flow
Phenomena (TSFP-8)
August 28 - 30, 2013 Poitiers, France

MERGING AND AUTO-GENERATION OF VORTICES IN WALL BOUNDED FLOWS

M.V. Goudar, W.P. Breugem, G.E. Elsinga
Laboratory for Aero & Hydrodynamics
Delft University of Technology
Leeghwaterstraat 21, 2628CA Delft, The Netherlands

ABSTRACT

For channel flow, we explore how a hairpin eddy may reach a threshold strength required to produce additional hairpins by means of auto-generation. This is done by studying the interaction of two eddies with different initial strengths (but both below the threshold strength), initial sizes and initial streamwise spacing between them. The numerical procedure followed is similar to Zhou *et al.* (1999). The two eddies were found to merge into a single stronger eddy in case of a larger upstream and a smaller downstream eddy placed within a certain initial streamwise separation distance. Subsequently, the resulting stronger eddy was observed to auto-generate new eddies. Merging of eddies thus is a viable explanation for the creation of the threshold strength eddies.

INTRODUCTION

In this work hairpin eddy model is used to explore the self-sustaining mechanisms of turbulence in the outer layer of wall bounded flows. Hairpin like vortices have been observed to populate the outer layer over a range of Reynolds numbers (Bandyopadhyay, 1980). Head & Bandyopadhyay (1981); Smith *et al.* (1984); Adrian *et al.* (2000) reported that these hairpins are organized in the direction of flow and occur in packets. Adrian *et al.* (2000) also reported that this vortex organization enhances the Reynolds shear stress which is related to turbulent drag. Ganapathisubramani *et al.* (2003) showed that the vortex packets in zero pressure gradient boundary layer flow contribute to more than 25% of the Reynolds shear stress ($-\langle u'v'\rangle$)[1] and occupy only 4% of the total area. So hairpin vortex organization in packets is considered to be important.

A possible explanation for packet formation is provided by a so-called auto-generation mechanism or parent-offspring concept. In this mechanism, a hairpin produces additional upstream (hairpin) vortices (see Haidari & Smith, 1994). Zhou *et al.* (1999) reported that only hairpins above a certain threshold strength can auto-generate.

In this study, we explore how such a hairpin of threshold strength may come into existence in the first place. This is done by studying the interactions between two ideal non auto-generating eddies in a direct numerical simulation (DNS). A variety of scenarios were created based on different initial strengths, initial sizes and initial streamwise spacing between the aligned eddies as shown in figure 1.

METHODOLOGY

Direct numerical simulation (DNS) of fully developed channel flow was carried out at $Re_\tau = 360$ (based on full channel height). Simulations were carried out on a computational domain non-dimensionalized w.r.t full channel height given by $2\pi \times 1 \times \frac{2}{3}\pi$ in streamwise, wall normal and spanwise directions. Uniform staggered grids with resolution of $808 \times 128 \times 272$ in x, y and z directions were used. Runge-Kutta third order scheme was employed for integration in time and central difference for spatial derivatives for solving Navier-Stokes equations. There was good agreement of flow statistics of the present data with the data of Kim *et al.* (1987).

An initial flow field with an eddy structure whose evolution will be studied is extracted from the DNS database of above fully developed turbulent channel flow by linear stochastic estimate (LSE). The initial velocity field is the sum of a turbulent mean profile ($\langle u_i(y)\rangle$) and a perturbation velocity ($\tilde{u}_i'(\mathbf{x}')$) associated to a conditional eddy. LSE is used to approximate the conditional averaged flow field $\langle \mathbf{u}'(\mathbf{x}')|\mathbf{u_e}(\mathbf{x})\rangle$ given an ejection ($u<0,\ v>0$) event. Here $\mathbf{u_e}(\mathbf{x})$ is a velocity event specified at point $\mathbf{x}$. The evolution of the eddy is studied by evolving the initial flow field in time in above DNS.

LSE

The procedure has been extensively discussed in Adrian (1994, 1996). LSE is the linear estimate of conditional average and is given by

$$\begin{aligned}\tilde{u}_i'(\mathbf{x}') &= \text{Linear estimate } \langle \mathbf{u}'(\mathbf{x}')|\mathbf{u_e}(\mathbf{x})\rangle \\ &= \sum_{j=1}^{3} L_{ij}(\mathbf{x}',\mathbf{x})u_j \quad i=1,2,3 \end{aligned} \tag{1}$$

where L_{ij} are linear estimate coefficients. L_{ij} is chosen such that the mean square error between the conditional average ($\langle \mathbf{u}'(\mathbf{x}')|\mathbf{u_e}(\mathbf{x})\rangle$) and $\tilde{u}_i'$ is minimum. This leads to the Yule-Walker equations given by

$$\sum_{j}^{3}\langle u_{ek}u_{ej}\rangle L_{ij} = \langle u_i'u_{ek}\rangle, \quad k=1,2,3.\ \ i=1,2,3. \tag{2}$$

[1] x,y,z and u,v,w (or u_1,u_2,u_3) represent streamwise,wall-normal and span-wise directions and velocities respectively. And velocity with $'$ e.g. u' is perturbation velocity. $\langle\ \rangle$ represents Reynolds average.

$\langle u_{ek}u_{ej}\rangle$ and $\langle u_i'u_{ek}\rangle$ represent the unconditional two-point correlations between the velocity event with the velocity event and the fluctuating velocity field with the velocity event respectively.

The final initial velocity field ($\tilde{u}_i$) for the two hairpin cases is given by a superposition of the mean flow and two conditional eddies :

$$\tilde{u}_i(\mathbf{x}') = \langle u_i(y)\rangle + \tilde{u}_i'(\mathbf{x}', \mathbf{u_{e1}}) + \tilde{u}_i'(\mathbf{x}' + \Delta x, \mathbf{u_{e2}}) \quad (3)$$

where perturbation velocity $\tilde{u}_i'(\mathbf{x}', \mathbf{u_{e1}})$ corresponds to the conditional eddy conditioned on the event $\mathbf{u_{e1}}$ and $\tilde{u}_i'(\mathbf{x}' + \Delta x, \mathbf{u_{e2}})$ conditioned on the event $\mathbf{u_{e2}}$ with a streamwise shift (Δx) from the former. Here $\mathbf{u_e}$ is given as $(\alpha u_m, \alpha v_m, \alpha w_m)$ where α represents the relative strength of the conditional eddy (Zhou *et al.*, 1999). In the present study, the velocity event $\mathbf{u_e}(\mathbf{x})$ is the value of a second quadrant (Q2) event ($u' < 0, v' > 0$) which maximizes the contribution to the Reynolds shear stress ($\langle u'v'\rangle$) at a particular location (y_e^+). That is, the value of u', v' which maximizes the product of $f_{uv}(u', v')$ with $u'v'$ in the second quadrant where $f_{uv}(u', v')$ represents the joint probability density function of occurrence of u' and v'. This maximum is denoted by u_m, v_m. If $w_e = 0$, then it is a symmetric event resulting in eddy shown in figure 2 and a non-symmetric event corresponds to $w_e \neq 0$ (see Zhou *et al.*, 1999, for further details).

Vortex Identification

Vortex identification is based on the local swirling strength suggested by Zhou *et al.* (1999). It is defined as the imaginary part (λ_{ci}) of a complex eigenvalue of a velocity gradient tensor. If all the eigenvalues are real then the local swirling strength is zero. Vortices are visualized by plotting the iso-surfaces of λ_{ci}^2 as shown in figure 2 for an eddy conditioned at $y_e^+ = 69$ and $\alpha = 2$.

RESULTS

The interaction between the two eddies is studied for occurrence of auto-generation by placing them aligned behind each other in the streamwise direction. Auto-generation as described in Zhou *et al.* (1999) means generation of new hairpin vortices from a parent hairpin vortex. In the present case, auto-generation is loosely referred to as the creation of new structures whether hairpins or a pair of counter-rotating quasi-streamwise vortices. An overview of the cases studied are listed in table 1. It is important to emphasize that all eddies shown in the table do not auto-generate individually in contrast to Parthasarathy (2011), who considered two strong above threshold strength eddies that auto-generate individually. The only exception to this rule is $(y_e^+, \alpha) = (68.9, 2)$ in cases II and III. It can be observed from the table that auto-generation occurs in both the cases of merging and no merging. In following sections we explore under what circumstances merging occurs and how it leads to auto-generation. The cause for merging is studied as the function of strength, spacing and event location. Also cases with no merging leading to auto-generation are briefly discussed. First, however single eddy cases are considered to validate our code and for later reference when comparing to the two eddy cases.

Single eddy case

Single eddy evolution is used as a baseline for studying interaction between two eddies. The initial conditional eddy is a single pair of lifted, counter-rotating streamwise vortices (Zhou *et al.*, 1999). The LSE procedure was validated by comparing present results with Zhou *et al.* (1999). The λ_{ci} value scaled with full channel height for $\alpha = 1$ at $y_e^+ = 46.4$ in present case was found to be 18.71 compared to 17.83 at $y_e^+ = 49.6$ in case of Zhou *et al.* (1999).

Few important observations connected with the evolution of an eddy from Zhou *et al.* (1999) and our studies are as following. All conditional eddies evolve into a hairpin vortex which is referred to as a primary hairpin (Zhou *et al.*, 1999). If the initial eddy has sufficient strength then the primary hairpin auto-generates. A conditional eddy based on lower event location (y_e^+), evolves slower into a hairpin as the shear layer roll up into a span-wise vortex is delayed due to the lower mean flow velocity. This shear layer is formed when ejected fluid between streamwise legs encounters the mean flow. Increasing the eddy strength α results in a higher initial swirling strength, which leads to faster development of the streamwise vortices into a primary hairpin. This is due to intense shear layer formation in between the legs and top of the streamwise vortices (Zhou *et al.*, 1999). A conditional eddy with a higher swirling strength travels at the same speed or slightly slower than an eddy with lower swirling strength at the same event location (y_e^+). A conditional eddy based on an event specified at higher event vector location (y_e^+) travels faster for the same swirling strength. This is because the mean flow velocity is higher at higher y_e^+.

Merging as function of event location

From table 1, it can be seen that merging is observed for the cases where an upstream eddy is at a higher event location compared to downstream eddy (case I and II). Cases III and IV with an upstream eddy at lower ejection event location compared to the downstream eddy, do not show any signs of merging. In case III and IV, the downstream eddy moves faster than the upstream eddy, because an eddy with the higher y_e^+ travels faster then the lower y_e^+ due to higher mean flow velocity. The reverse also happens in cases I and II, where the upstream eddy travels faster and catches up with the eddy downstream till they merge. Such a scenario has been observed experimentally in a turbulent boundary layer by Elsinga *et al.* (2012).

Merging as function of spacing

Merging as a function of initial streamwise spacing is studied for case I, where the strength of the upstream eddy was higher than the downstream eddy. From table 1, it can be observed that merging occurs when two eddies are separated by initial streamwise distance $\Delta x^+ < 140.6$. For the cases with initial streamwise spacing $\Delta x^+ = 281.2$ & 421.9, there is no merging. For the initial streamwise separation $\Delta x^+ = 140.6$ (see figure 3b), merging is happening, and at the same time the strength of the downstream eddy is reducing (nearly vanishing). Also the downstream eddy does not vanish when simulated as a single eddy case. So a stronger eddy upstream influences the weaker eddy downstream by pulling it towards itself. This leads to thinning and stretching of the downstream eddy.

Table 1: Overview of simulations of the cases with two eddies.

Case	Ref Plane (y^+_{e1}, y^+_{e2})	Strength $(\alpha_1,\ \alpha_2)$	Δx^+	Max λ^2_{ci}	Position (y/H)	Auto-generation	Merging
I	(102.7,68.9)	(2,1)	70.3	331.36	0.2617	Yes	NA
I	(102.7,68.9)	(2,1)	101	328.08	0.2695	Yes	Yes
I	(102.7,68.9)	(2,1)	140.6	333.75	0.2695	Yes	Yes
I	(102.7,68.9)	(2,1)	281.2	336.12	0.2695	Yes	No
I	(102.7,68.9)	(2,1)	421.9	343.06	0.2695	No	No
II	(102.7,68.9)	(1,2)	70.3	690.37	0.1758	Yes	NA
II	(102.7,68.9)	(1,2)	140.6	688.10	0.1758	Yes	Yes
III	(68.9,102.7)	(2,1)	140.6	738.52	0.1758	Yes	No
III	(68.9,102.7)	(2,1)	281.2	691.15	0.1758	Yes	No
IV	(68.9,102.7)	(1,2)	140.6	371.37	0.2617	Yes	No
IV	(68.9,102.7)	(1,2)	281.2	348.14	0.2695	No	No

Merging as function of strength

Initial streamwise spacing was fixed and the strength of the eddies was varied. Case I (fig 3b) and case II (fig 3c) with the same initial streamwise spacing $\Delta x^+ = 140.6$ between eddies was considered. In case II, there was a quicker and clear merging of the two eddies. Unlike the case I, the strength of the downstream eddy does not strongly reduce and vanish in case II. The downstream eddy is stronger in case II compared to case I, hence it takes more time before its strength diminishes allowing merger over a larger separation distance. These observations suggest that the distance between the eddies may be more then $\Delta x^+ = 140.6$ for merging to occur in case II. Also the eddies are pulled closer to each other much faster in case II. This may be because of higher strength in downstream eddy means lower mean velocity locally as the ejection ($u' < 0$) is stronger. This leads to slow down of downstream eddy and hence faster merging.

To summarize the above sections on vortex merging:

- Merging occurs when a eddy of higher event location is upstream to an eddy of lower event location.
- There is certain distance between the eddies within which a merger can occur like $\Delta x^+ < 140$ in case I.
- Merging is also dependent on the strength of eddies. It is faster when the strength of the smaller downstream eddy is higher.
- After merging the geometric shape of the structure remains broadly similar (i.e, hairpin-like see figure 3a at $t^+ = 43.2$).

Auto-generation after merging

The initial condition of case I contains two eddies which do not auto-generate individually. But when they are put together, new structures are generated which can be seen in figures 5a, 5b, 5c and 5d. In case II and III, one of the two eddies $(y^+_e, \alpha = 68.9, 2)$ auto-generates individually. This single eddy evolution is shown in figure 6e for comparison. Figures 6a, 6b and 6c show the cases with two eddies where one eddy auto-generates individually. In these cases, formation of a tertiary eddy upstream can be observed in figures 6a and 6c. So compared to the single eddy case (figure 6e) which doesn't reveal a tertiary eddy, there is an enhancement in terms of generation of new structures. From the results presented in figures 5 and 6, it can be inferred that there is an interaction between two eddies when aligned behind each other which leads to the generation of new structures. And also, the auto-generation can take place when two eddies which individually do not possess sufficient strength to auto-generate are aligned behind each other.

Figures 5a, 5b, 5c and 5d show the effect of spacing on the generation of new structures. As the streamwise distance (Δx^+) is increased from 70.3 to 421.9, the newly generated streamwise vortices upstream are weaker. So with increasing Δx^+, the interaction which causes auto-generation weakens. This also suggests that the two eddies become independent of each other as the spacing between the two grows. Merging takes place for the streamwise spacing $\Delta x^+ = 70.3,\ 101$ and 140.6 (70.3 is an initial merged case) and also auto-generation occurs. Hence merging results in formation of stronger eddies of threshold strength. It can also be noted that the auto-generation occurs after merging, so there is no vortex-vortex interaction in these cases. Hence process of auto-generation and merging are separated in time.

From figure 5, it can also be observed there is no remarkable change in generation of new structures as streamwise spacing is increased. So merging do not influence the trend of decreasing size of new structures with increasing streamwise spacing. The vortex-vortex interaction decreases with increasing streamwise spacing but still there is an interaction which can be seen in case of larger separation distance. This may be because both the eddies share the same low speed streak, due to which fluid ejected by downstream eddy is absorbed by upstream eddy. This could be

described as vortex-streak interaction.

Figure 4 represents the evolution of maximum λ_{ci}^2 for the case I $(y_{e1}^+, y_{e2}^+) = (102.7, 68.9)$ with different streamwise spacing (Δx^+) and a single eddy case corresponding to $(y_e^+, \alpha) = (102.7, 2)$ for comparison. In this figure, it can be observed that the amplification of normalized maximum λ_{ci}^2 with time, decrease as streamwise spacing Δx^+ increases. A sudden shift in the location of the max λ_{ci}^2 from the head to legs is observed. The time at which this shift takes place is marked by the dot '•' shown in the figure. The first maximum λ_{ci}^2 (associated to the head) has a peak value of 5.09 for streamwise spacing $\Delta x^+ = 70$ which is twice the value 2.7 in the single eddy case. For $\Delta x^+ = 101$, 140.6, 281.2 and 481.9 the peak value of maximum λ_{ci}^2 is 3.61, 2.93, 2.83 and 2.78 respectively. From the single eddy simulations, it was observed that the higher the initial growth rate the faster is the development of an initial eddy into a primary hairpin. So it can be implied that the primary hairpin formation takes longer as the spacing between eddies is increased, as growth rate decreases with increasing spacing. This is consistent with the earlier 3-d observations.

After the point '•', the location of normalized maximum square of swirling strength (λ_{ci}^2), shifts to the legs of streamwise vortex. The maximum λ_{ci}^2 in the legs for the case of $\Delta x^+ = 70.3$, 101 and 140.6, increases and reaches peak values of 5.67, 5.09 and 4.27 respectively. Compared to the single eddy case the relative increase in max λ_{ci}^2 is much higher in case of the legs than in the head. For other streamwise spacing i.e, the non merging cases, after point '•' maximum λ_{ci}^2 continues to decrease. As new structures from auto-generation are formed near the legs, a strong amplification of λ_{ci}^2 in the legs is expected to enhance the formation of new structures, which is consistent with the present observations (figure 5).

Auto-generation: Non merging cases

For case III, where there is no merging for $\Delta x^+ = 140$, tertiary hairpin formation occurs (see figure 6c at $t^+ = 349.2$). The second eddy $y_e^+ = 102.7$ (eddy 2) remains as a downstream vortex and becomes stronger which can be seen by its increased size in figure 6c. For $\Delta x^+ = 281$, a new downstream eddy (located in between the two initial eddies) is created by the initial upstream eddy $y_e^+ = 68.9$ (eddy 1) as shown in figure 6d at $t^+ = 248.4$. This newly generated structure interacts with the second initial eddy downstream $y_e^+ = 102.7$ and becomes a hairpin as shown in figure 6d at $t^+ = 349.2$ which otherwise was just a pair of counter-rotating streamwise vortices (see figure 6e). Hence there is an enhancement of auto-generation even when two eddies do not merge.

From all these observations, it may be inferred that, vortex-vortex and vortex-streak interactions happen when the streamwise spacing is sufficiently small. And vortex-streak interaction occurs when the separation distance is larger. Regardless merging or not, the interactions tend to promote auto-generation.

CONCLUSIONS

Two non auto-generating eddies were found to merge into a single stronger eddy when a larger (larger y_e^+) upstream and a smaller (lower y_e^+) downstream eddy are placed within a certain initial streamwise distance. The larger eddy travels faster due to the higher mean velocity farther from the wall and merges with the smaller eddy. An example is shown in figure 3a. This is consistent with the experimental observations by Elsinga *et al.* (2012). The resulting stronger eddy was subsequently observed to auto-generate new eddies (figure 5b).

Figure 4 shows the variation of the maximum normalized λ_{ci}^2 with time for different initial spacing between the vortices. In this case an eddy with higher y_e^+ and high strength was upstream of a lower y_e^+ eddy of low strength. From the figure, it can be observed that there is an amplification in maximum normalized λ_{ci}^2 in cases with merging compared to the single eddy case. Furthermore, the location of the maximum λ_{ci}^2 was found to shift suddenly from the head to the legs. The time at which it occurred is indicated by '•' in figure 4. The effect of merging was observed to be even stronger in the legs when compared to the head; the second peak (after '•') increases from about 2.0 for the single eddy case to nearly 5.7 for two merging eddy initially at $\Delta x^+ = 70$. This strong increase in strength and the observation of generation of new structures near the legs in the merged cases suggests that the higher swirling strength in the legs lead to instability which results in creation of new structures.

In some cases, new structures were generated even though there was no merging and the streamwise spacing was large. So there has to be another kind of interaction which results in auto-generation, as a direct vortex-vortex interaction weakens with increasing spacing. This interaction may be between the low speed streak and the upstream vortex, as both the eddies share the same low speed streak.

Merging of eddies thus is a viable explanation for the creation of threshold strength eddies. Moreover, it extends the auto-generation process towards a possible self-sustaining mechanism: two initial hairpins merge producing a strong hairpin, which further creates a new hairpin structure by auto-generation resulting again in two hairpins. Low speed streaks may also play a role in the generation of new structures, but this aspect is still under study. Hence the criterion and the mechanisms to determine the auto-generation become more complex, when two hairpins are aligned behind each other than the one mentioned (threshold strength) for a single eddy case in Zhou *et al.* (1999).

REFERENCES

Adrian, R. J. 1994 Stochastic estimation of conditional structure: a review. *Applied Scientific Research* **53**, 291–303.

Adrian, R. J. 1996 Stochastic estimation of the structure of turbulent fields. In *Eddy structure identification* (ed. J. P Bonnet), *CISM International Centre for Mechanical Sciences* 353, pp. 145–196. Springer-Verlag.

Adrian, R. J., Meinhart, C. D. & Tomkins, C. D. 2000 Vortex organization in the outer region of the turbulent boundary layer. *Journal of Fluid Mechanics* **422**, 1–54.

Bandyopadhyay, P. 1980 Large structure with a characteristic upstream interface in turbulent boundary layers. *Physics of Fluids* **23**, 2326.

Elsinga, G. E., Poelma, C., Schröder, A., Geisler, R., Scarano, F. & Westerweel, J. 2012 Tracking of vortices in a turbulent boundary layer. *Journal of Fluid Mechanics* **697**, 273–295.

Ganapathisubramani, B., Longmire, Ellen K. & Marusic, Ivan 2003 Characteristics of vortex packets in turbulent

boundary layers. *Journal of Fluid Mechanics* **478**, 35–46.

Haidari, A. H. & Smith, C. R. 1994 The generation and regeneration of single hairpin vortices. *Journal of Fluid Mechanics* **277**, 135–162.

Head, M. R. & Bandyopadhyay, P. 1981 New aspects of turbulent boundary-layer structure. *Journal of Fluid Mechanics* **107**, 297–338.

Kim, J., Moin, P. & Moser, R. 1987 Turbulence statistics in fully developed channel flow at low Reynolds number. *Journal of Fluid Mechanics* **177**, 133–166.

Parthasarathy, P. K. 2011 Dynamics of vortices in numerically simulated turbulent channel flow. Master's thesis, Arizona State University, USA.

Smith, CR, Patterson, GK & Zakin, JL 1984 A synthesized model of the near-wall behavior in turbulent boundary layers. *NASA STI/Recon Technical Report N* **84**, 19764.

Zhou, J., Adrian, R. J., Balachandar, S. & Kendall, T. M. 1999 Mechanisms for generating coherent packets of hairpin vortices in channel flow. *Journal of Fluid Mechanics* **387**, 353–396.

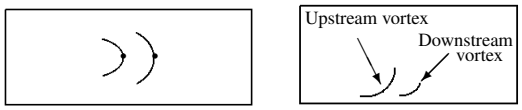

(a) Top view of two vortices aligned in streamwise direction. Distance between '•' is the streamwise spacing between two vortices given by Δx^+.

(b) Side view of two vortices with higher strength & higher y_e^+ upstream and lower strength & lower y_e^+ downstream, respectively. y_e^+ denotes y^+ value of reference plane for conditional eddy.

Figure 1: Scenarios showing the arrangement of eddies in the initial condition for DNS

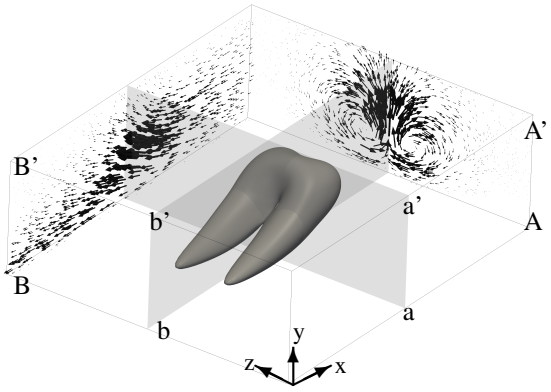

Figure 2: Initial condition showing conditional eddy for $y_e^+ = 69$ and $\alpha = 2$. Conditional eddy is isosurface of $\lambda_{ci}^2 = 33$, which is 5% of the maximum λ_{ci}^2. Vector plots correspond to in plane perturbation velocities. Vector plot on plane aa' and bb' is translated to plane AA' and BB' respectively for better visualization.

(a) Case I, $\Delta x^+ = 101$. At time (from left to right) $t^+ = 0$, 14.4, 28.8, 43.2

(b) Case I, $\Delta x^+ = 140.6$. At time (from left to right) $t^+ = 0$, 14.4, 28.8, 43.2, 50.4, 57.6, 64.8

(c) Case II, $\Delta x^+ = 140.6$. At time (from left to right) $t^+ = 0$, 14.4, 28.8, 36.0, 50.4

Figure 3: Sequence showing the merging of vortices

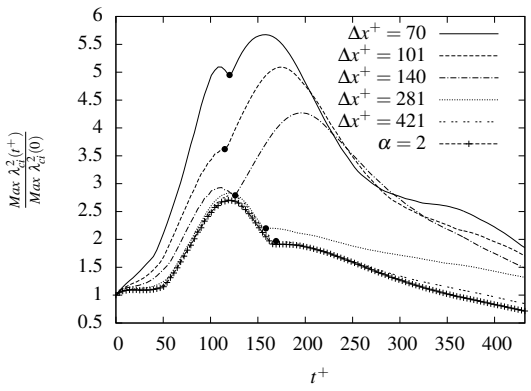

Figure 4: Temporal evolution of the normalized maximum of λ_{ci}^2 for different initial streamwise separation (Δx^+). This is for the case of a large vortex ($y_e^+ = 103,\ \alpha = 2$) upstream of a smaller one ($y_e^+ = 69,\ \alpha = 1$). The time at which the location of maximum λ_{ci}^2 shifts from the head to the streamwise vortex legs is indicated the '•'. $\alpha = 2$ represents single eddy case at $y_e^+ = 103$.

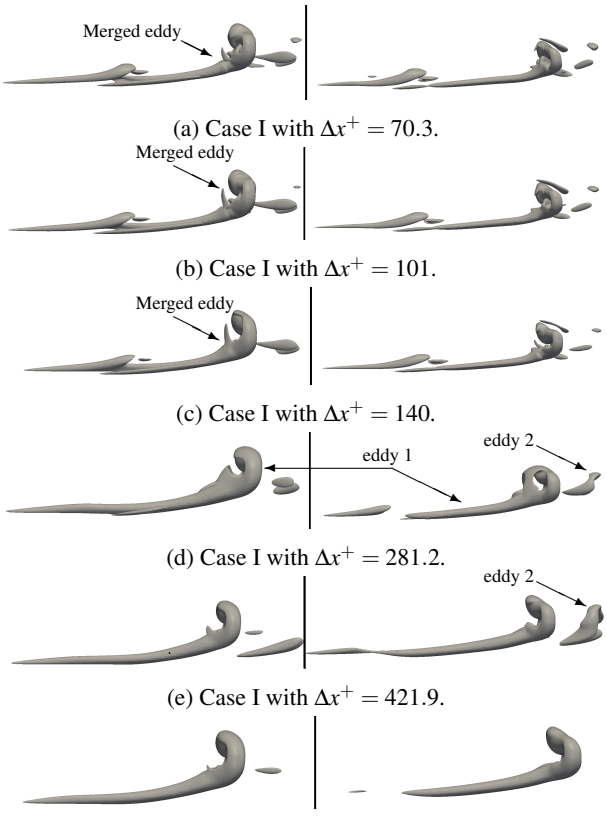

(a) Case I with $\Delta x^+ = 70.3$.

(b) Case I with $\Delta x^+ = 101$.

(c) Case I with $\Delta x^+ = 140$.

(d) Case I with $\Delta x^+ = 281.2$.

(e) Case I with $\Delta x^+ = 421.9$.

(f) Simulation of single eddy $(y_e^+, \alpha) = (102.7, 2)$.

Figure 5: Side view of different auto-generation cases (case I) when eddies are aligned behind each other compared to the case of single eddy ($y_e^+ = 102.7$). The effect on auto-generation due to spacing between them is studied. All eddies are visualized by iso-surface of $\lambda_{ci}^2 = 30$. Left column is at $t^+ = 248.4$ and right column is at $t^+ = 349.2$.

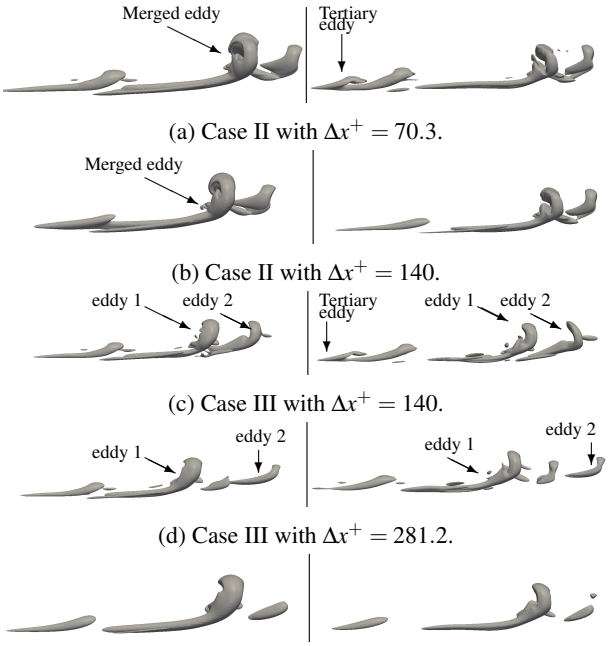

(a) Case II with $\Delta x^+ = 70.3$.

(b) Case II with $\Delta x^+ = 140$.

(c) Case III with $\Delta x^+ = 140$.

(d) Case III with $\Delta x^+ = 281.2$.

(e) Simulation of single eddy $(y_e^+, \alpha) = (68.9, 2)$.

Figure 6: Side view of different auto-generation cases (case II & III) when eddies are aligned behind each other compared to the case of single eddy ($y_e^+ = 68.9$). All eddies are visualized by iso-surface of $\lambda_{ci}^2 = 30$. Left column is at $t^+ = 248.4$ and right column is at $t^+ = 349.2$.